Journal of Applied Electrochemistry (2005) 35:699–708
DOI 10.1007/s10800-005-1364-x
© Springer 2005

Development of an optical fiber monolith reactor for photocatalytic wastewater Treatment

HONGFEI LIN and KALLIAT T. VALSARAJ*
Gordon A. and Mary Cain Department of Chemical Engineering, Louisiana State University, Baton Rouge, LA, 70803, USA
*(*author for correspondence, e-mail: valsaraj@lsu.edu; phone: +225-578-1476; fax: +225-578-1476)*

Received 17 November 2004; accepted in revised from 10 January 2005

Key words: dichlorobenzene, optical fiber monolith reactor, phenanthrene, photocatalysis, TiO_2 film, water treatment

Abstract

A photocatalytic reactor, which employs a ceramic multi-channel monolith as a support for TiO_2 and bare quartz fibers inserted inside the monolithic channels as both a light-transmitting conductor and a support for TiO_2, was constructed and tested for water treatment by investigating the photocatalytic degradation of *o*-dichlorobenzene (DCB) and phenanthrene (PHE). This configuration provides a higher surface area for catalyst coating per unit reactor volume compared to the continuous annular reactor (CAR) and optical fiber reactor (OFR). The light distribution profile inside each cell of the monolith is analyzed. Exponential decay of light was observed in propagation along the quartz fiber core and penetration into the TiO_2 film. Optimum thickness of TiO_2 layer on the optical fiber was found to be ≈ 0.4 μm in this study. The kinetics of DCB and PHE degradation were pseudo-first order. The effect of the water flow velocity was investigated and showed that the operation was in the mass transfer control regime. Overall rate constants were extracted from the experimental data; and these were then used to calculate the apparent quantum efficiency of photocatalytic degradation. Greater apparent quantum efficiency was observed for the optical fiber monolithic reactor (OFMR) compared with that of the CAR.

1. Introduction

Heterogeneous photocatalysis using low energy UV irradiated TiO_2 has been shown to be an effective means of removing organic pollutants from water streams [1–6]. Crucial insight into the mechanism of the photocatalysis has been obtained and the use of these processes has been demonstrated on a practical level. However, there are still a number of challenges that prevent it from being used as a large-scale process [7]. The selection of an appropriate catalyst configuration is of utmost importance in a large-scale reactor to provide a large amount of activated photocatalyst per unit volume of liquid treated without loss of the processing capability for the reactor. The majority of photocatalytic reactors are a variation of the annular reactors in which the catalyst is coated on the reactor wall [8, 9], lamp casing [10] or different support substrates such as glass beads [11, 12], plates [13], and mesh [14]. All these reactor designs are limited to the laboratory scale due to low light utilization efficiencies and mass transport limitations. In order to meet this reactor design challenge, a fixed-bed like system that employs a bundled optical fiber cable array was developed.

Marinangeli and Ollis [15–17] first proposed that optical fibers could be used for both remote light transmission and as a solid support for photocatalysts. Experimental application of the idea was demonstrated by Hofstadler et al. [18] who designed a TiO_2-coated quartz fiber reactor and used it in the photodegradation of 4-chlorophenol in water. Peill and Hoffmann [19–21] developed, characterized, and modeled an optical fiber reactor (OFR) system for photomineralization of pentachlorophenol, 4-chlorophenol, dichloroacetate and oxalate in water. Similar batch-type OFR systems were easily devised to use for the photocatalytic degradation of gaseous organic pollutants such as benzene or acetone in air streams [22, 23]. The OFR system enhances the uniformity and distribution of the UV light within a given reaction volume and allows for the remote delivery of light and thus can be used for the *in situ* treatment of contaminated sites in the environment. However, immobilization of TiO_2 on an optical fiber also creates its own problems. In an OFR system, since the contaminant diffusion direction is opposite to the light transmission direction, the charge carriers can be generated relatively far from the liquid–catalyst interface and, consequently, are more susceptible to recombination loss [22]. Also the internal mass transfer

resistance within the TiO_2 film further lowers the overall reaction rate. Another drawback of an OFR reactor is that the configuration does not effectively utilize the entire reactor volume. The optical fibers usually take up 20–30% of the reactor volume but provide relatively low surface area of the coating support since the optical fiber is usually thin.

On the other hand, as a unique catalyst support, a honeycomb monolith, which contains a large number of small channels in parallel through which the reacting fluid flows and the catalyst is deposited on the walls of the monolithic channels, can provide a high surface-to-volume ratio and allow high flow rates with low pressure drop. Moore et al. [24] found that a honeycomb monolith substrate has 10–100 times higher specific surface area than that of plates and beads type substrates with the same outer dimensions. Moreover, the monolithic reactor is easy to scale-up by increasing the number of channels. Several monolithic reactors were used in the treatment of air streams by photocatalysis [25–28]. However, the efficiency of these reactors was hindered since limited UV light could penetrate through the cells of the honeycomb substrate.

In this study, a photocatalytic reactor with distributed optical fibers inside a ceramic monolithic structure was constructed and tested. Thin TiO_2 films were coated on the outer surface of the stripped optical fibers that allowed the UV light to radially refract out of the fibers. Moreover, thick TiO_2 films were formed on the inner surface of monolith channels, which can be illuminated by the refracted UV light out of the optical fibers. This configuration combined the advantages of the monolithic reactor and the optical fiber cable reactor. The higher surface area of the illuminated catalyst in the given reactor volume compensated for some loss of UV light due to the absorption and scattering by the organic pollutants in the wastewater. Thus, a higher overall reaction efficiency may be reached. We chose 1,2-dichlorobenzene (DCB) and phenanthrene (PHE) as the model contaminants in water as we did in preliminary work using conventional reactors [29, 30]. Experiments were performed under conditions relevant to the evaluation of the design of the optical fiber monolith reactor. A comparison of the overall degradation efficiencies of the present reactor with those of a batch slurry reactor and a continuous annular reactor was made to test the feasibility of the reactor.

2. Experimental

2.1. *Materials*

DCB of 98% purity was obtained from EM Sciences, Gibbstown, NJ. Phenanthrene of 98% purity was obtained from Aldrich Chemicals, Milwaukee, WI. Powered titania (P25) donated from Degussa Corporation, Akron, PA was used as the photocatalyst. The TiO_2 crystallites had a mean surface area of 60–70 $m^2\ g^{-1}$, a mean particle diameter of 20 nm and the point of zero charge at a pH of 6.8.

2.2. *Characterization of TiO_2 coating*

A dip-coating method was used to immobilize TiO_2 particles on the outer wall of the quartz optical fiber and the inner walls of the monolith substrate. TiO_2 suspensions in deionized water were prepared and dispersed by sonication and magnetic stirring. The adhesion of TiO_2 particles to quartz is primarily through electrostatic interactions. TiO_2 suspensions of 0.25, 0.50, 1, and 2 wt. % were used to coat the optical fibers, while a 20 wt. % suspension was used to coat the monolith channels. Multimode quartz optical fibers (3M Power-Core FT-400-UMT) with a diameter of 400 μm were purchased from Thorlab, Newton, NJ. The optical fiber wire was cut to multiple equal-length pieces and individual fiber was stripped for the desired length. Firstly, the fiber was completely stripped of its protective buffer using a wire stripper and secondly, the inner polymer cladding was removed with a fine sand paper. Finally they were wiped with a soft tissue soaked in acetone. After these procedures, the quartz core was completely exposed and the surface was roughened to facilitate deposition of TiO_2 particles. The exposed quartz core was dipped into a well-stirred TiO_2 slurry solution for 10 min, and then air-dried at 260 °C for 30 min using a heat gun. The dip-drying procedure was repeated twice followed by rinsing with plenty of deionized water in order to wash out the loosely bound TiO_2 particles. The coated fiber was then air-dried at room temperature for 24 h. Selected coated optical fibers were cut into several 1-cm pieces and gold-coated by using a sputter coater for determination of thickness and surface roughness of the TiO_2 film by scanning electron microscopy (SEM) (Cambridge Model S-360). Dip-coating the monolith channels was similar to that on the optical fibers except that the TiO_2-coated monolith block was fired in a furnace at 300 °C for 1 hour.

2.3. *Multi-channel optical fiber monolith reactor*

The experimental assembly for the multi-channel photocatalytic monolith reactor is shown in Figure 1. The reactor consists of a light source, a coated optical fiber bundle, a coated multi-channel monolith block, a reaction vessel and a reservoir. The main body is a ceramic honeycomb monolith with 61 cylindrical channels obtained from Applied Ceramics, Atlanta, GA. The length of the monolith block is 30 cm with a channel diameter of 3 mm. The multiple cylindrical channels were coated on the inside with TiO_2 using the dip-coat method. Then the coated monolith block was placed inside a cylindrical stainless steel container fabricated with flanges at either end. One TiO_2-coated fiber was inserted through each channel in the monolith. Every channel was thus an independent reaction unit. Each fiber passes

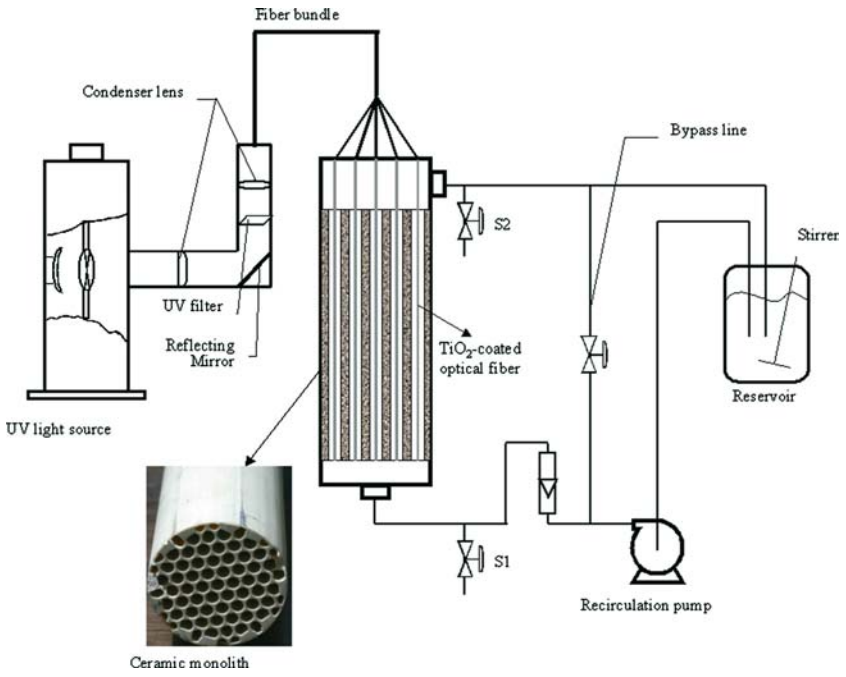

Fig. 1. A schematic of the optical fiber monolith reactor assembly and experimental setup. The reactor was operated in the continuous recycle mode. Samples were taken at S1 and S2 to determine the overall removal efficiency.

through perforated plates at the top and bottom of the cylindrical monolith, thus maintaining their center position in each flow channel. The head cover on the top end was attached with provisions for fluid inlet and fiber optic passage. The prepared optical fibers with the monolithic reactor were then sent to Fused Fiber Optics, LLC, PA for bundling and polishing.

A 500 W Xe short arc lamp, which was obtained from Spectral Energy Corporation, NY, was used as the UV radiation source. Light was delivered to the fiber optic bundle from the UV light source, through a collimator, a reflecting mirror, a UV band pass filter (280–380 nm), a condenser lens and finally focused on the polished end of the fiber optic bundle. Adjusting the relative position of the condenser lens and the reflecting mirror we can obtain various incident angles. The influent feed stream was pumped into the reactor in an upflow mode and then recycled through the reactor after mixing in the reservoir. The solution in the reservoir was well mixed by magnetic stirring. Thus the overall operation was in the continuous recycle mode with multiple passes through the reactor. The volume of the reservoir was 900 ml. The inlet and outlet samples were collected at valve ports S1 and S2 respectively. The bypass line from the outlet of the pump to the reservoir was used to adjust the flow rate of the water stream passing the reactor. Samples were collected in 2 ml vials with a cap and septum.

2.4. *Methodology and analysis*

The DCB or PHE solution was recirculated through the reactor in the dark (i.e., without UV light) for 2 h to ensure that adsorption equilibrium was reached. At 2 h the UV lamp was turned on. The decline in the concentration of DCB or PHE in the reservoir was obtained by periodic analysis of the aqueous phase and the overall reaction loss of DCB or PHE was obtained by sampling the influent and effluent at 10–20 min intervals. The DCB in the aqueous sample was analyzed using a Hewlett-Packard gas chromatograph (Model HP 5890 Series I) coupled with a mass spectrometer (HP 5971). Details of the analysis were given in our previous paper [29]. The PHE in the aqueous sample was analyzed using a Hewlett-Packard High Performance Liquid Chromatograph (HP 1100). The UV light intensity was measured by a UV radiometer (UVP UVX radiometer) coupled with a 365 nm sensor (UVX-36 long wave sensor).

3. Results and discussion

3.1. *Thickness of the coated optical fiber*

SEM images of TiO_2 layer on a quartz optical fiber that was coated with 0.25, 0.5, 1.0, 2.0 wt. % TiO_2 slurry solutions are compared in Figure 2 (cross-sectional view), which indicates that the thickness of TiO_2 layer was uniform around the surface of the fiber. As shown in Figure 3, the thickness was found to be 0.4–1.7 μm for TiO_2 layers generated from slurry solutions containing 0.25–2 wt. % of TiO_2. The thickness of the TiO_2 layer formed on the surface of the fiber increased almost linearly with increasing TiO_2 content in aqueous solution from which the dipping was carried out.

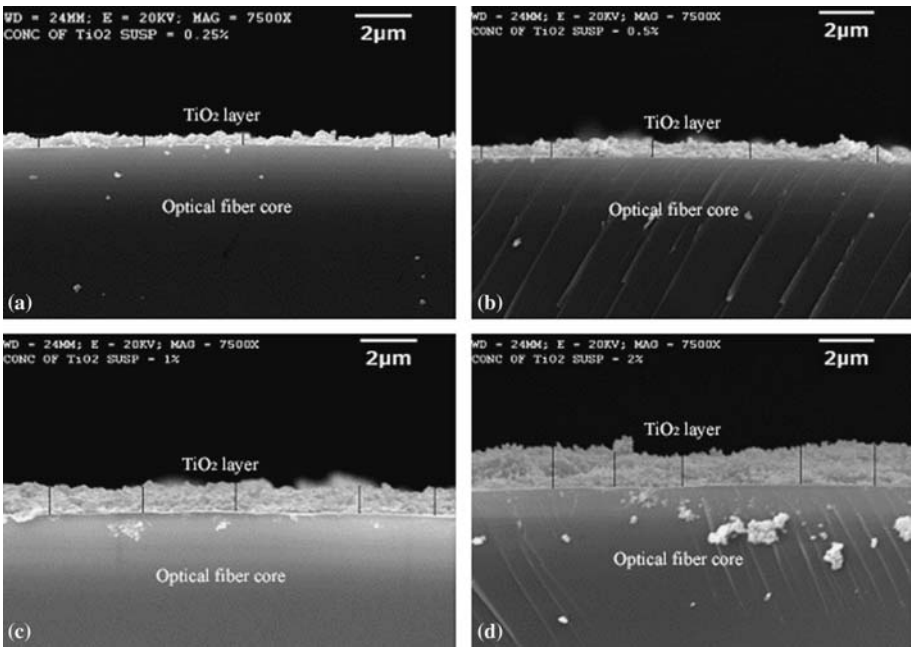

Fig. 2. SEM images of TiO_2 layer on a quartz optical fiber that was coated with (a) 0.25 wt. %; (b) 0.5 wt. %; (c) 1.0 wt. %; (d) 2.0 wt. % TiO_2 slurry solutions.

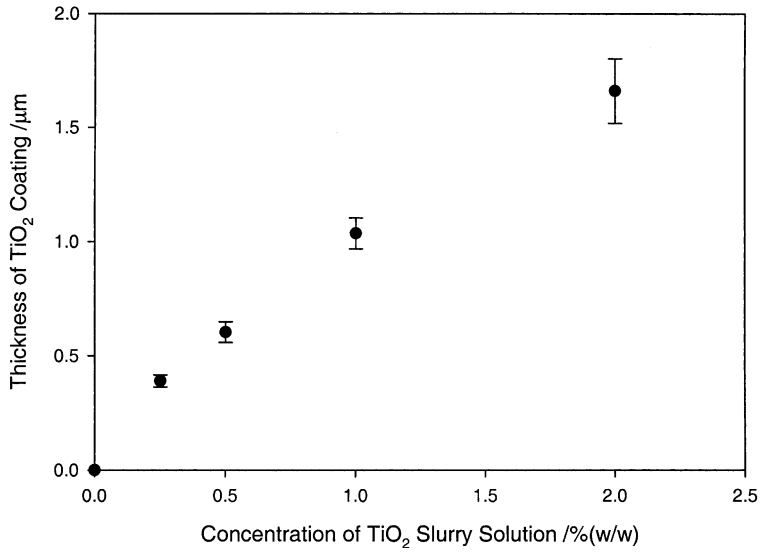

Fig. 3. Thickness of TiO_2 coating on optical fibers with O.D. 400μm versus concentration of TiO_2 slurry solution from which optical fibers were dip-coated.

3.2. *Kinetics of photodegradation of DCB and PHE in the monolith photocatalytic reactor*

The photocatalytic degradation rate of DCB or PHE depends on the concentration of adsorbed reactant and may be explained using the Langmuir–Hinshelwood kinetics [29, 30]. The monolith photocatalytic reactor was operated in a semi-batch mode with continuous recycle of the feed solution. A known volume of the feed solution was stored in the reservoir. The effluent from the reactor was mixed with the feed solution in the reservoir and recirculated through the reactor. The conversion in the reactor was used to obtain the overall reaction rate constant [29, 30],

$$k^* = -\frac{u}{L_e}\ln(1-x) \tag{1}$$

where u is the superficial liquid velocity (cm min^{-1}); L_e is the effective reactor length; x is the conversion of the reactant. The overall rate constant derives from two contributions, an external mass transfer from the liquid phase to TiO_2 coating and an intrinsic reaction rate:

$$\frac{1}{k^*} = \frac{1}{kK} + \frac{1}{k_m a_v} \quad (2)$$

where k_m is the mass transfer coefficient (cm min^{-1}), and a_v the surface area of TiO_2 per unit volume of the reactor (cm^2 cm^{-3}).

Figure 4a and 4b show the PHE and DCB concentration in the exit and inlet streams as well as the overall removal efficiency as a function of reaction time. The optical fiber was coated with 0.25 wt. % TiO_2 sol and the thickness of the TiO_2 film was approximately 0.4 μm, which is comparable with the wavelength of UV-A light. The monolith channel was coated with 20 wt. % TiO_2 sol and the thickness of the TiO_2 film is approximately larger than 10 μm which can fully absorb the incident light. Based on our observation, although the total length of the coated fiber is 30 cm, the light is almost extinct after 5 cm from the top. Therefore, the effective reactor length is only 5 cm and the residence time is about 2.16 min at the given flow velocity v = 2.314 cm min^{-1}. At 120 min the number of the passes through the reactor is approximately 55. The overall removal of DCB per pass from water remained constant and the process is therefore at quasi-steady state. For DCB, a steady-state conversion of about 17.8% was obtained under the same condition of flow velocity, v = 2.314 cm min^{-1} and at an initial concentration C_0 = 147 mg l^{-1}. The conversion of PHE was about 11.9% under the same conditions except the initial concentration was 505 μg l^{-1}. The faster conversion rate of DCB was evident even though the initial concentration of DCB was much higher. The low conversion in both cases was a result of the inadequate use of the reactor volume as mentioned earlier since only 5 cm of the reactor was effective in light transmission from the fiber. If the entire reactor length (30 cm) were available for reaction, the actual conversion would be 69 and 53% for DCB and PHE, respectively.

3.3. *Effects of feed concentration*

The initial concentration of the pollutant is always an important parameter in process water treatment through photocatalysis since the initial concentration affects the

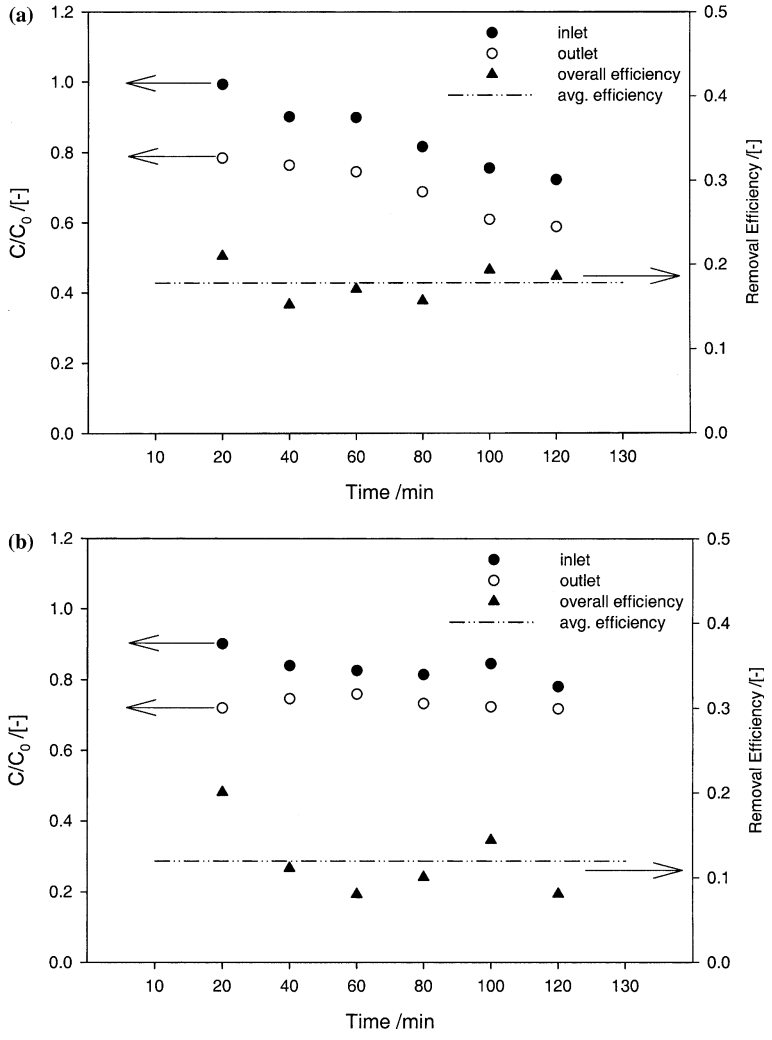

Fig. 4. DCB and PHE concentration in the outlet and inlet streams as well as the overall removal efficiency as a function of time. (a) DCB; (b) PHE. The flow velocity was 2.31 cm min^{-1}; the optic fibers were coated with 0.25 wt. % TiO_2 slurry solution.

coverage on the catalyst surface. The kinetic expression is of the Langmuir type. When the initial concentration of the pollutant is high, the surface of the active catalyst will be saturated by the reactant. Thus the Langmuir-type kinetic rate expression reduces to a zero-order rate expression and the overall rate would not depend on external mass transfer, i.e., be kinetically limited. The concentration versus time will follow a linear relationship. On the other hand, when the initial concentration of the pollutant is very low, the kinetic rate expression becomes a pseudo-first order. In this case, the overall rate would certainly depend on mass transfer and the initial concentration would not affect the conversion rate. Our previous paper [30] concluded that the saturation adsorption capacity for PAHs on TiO_2 was never reached since the solubility of PAHs in the aqueous solution is too small based on the experimental data in an annular continuous reactor. The effect of PHE concentration between 16.7 and 747 $\mu g\ l^{-1}$ upon fractional conversion is shown in Figure 5 at a fixed feed velocity of 2.87 cm min^{-1} in the monolith reactor. The independence of the PHE fractional conversion on initial concentration was confirmed regardless of the different reactor configuration. This also suggested the necessity to improve the mass transfer behavior in the monolith reactor to get better overall degradation efficiency.

3.4. *Effects of mass transfer*

Organic compounds must diffuse from the bulk liquid through a boundary layer to reach the liquid–catalyst interface, i.e., external mass transfer. Organic compounds must then migrate through the catalyst layers (diffusion within the catalyst film) to find active surface sites where they adsorb and eventually react. The mass transfer process through the catalyst layer is similar to interparticle diffusion and is defined as an internal mass transfer process. It should be noted that TiO_2 catalyst particles are non- porous, and therefore intraparticle diffusion is absent. The internal mass transfer is an intrinsic property of the catalyst film, and is determined by the nature of the catalyst, coating porosity, and the thickness of the catalyst film. Internal mass transfer can be negligible if the catalyst film is very thin. On the other hand, increasing the flow velocity (Reynolds number) over the immobilized catalyst could reduce the external mass-transfer resistance. The extreme case is that the external mass transfer limitation is overcome at high flow velocity and the conversion is limited only by the intrinsic reaction rate, which is independent of flow velocity. For this we turn to Equation (2), which represents the magnitude of external mass transfer and intrinsic reaction terms on the overall rate constant. Equation (2) shows that the overall resistance to conversion ($1/k^*$) is the sum of the mass transfer resistance ($1/k_m a_v$) and that due to intrinsic reaction ($1/kK$). The intrinsic reaction term is independent of feed velocity [29–32]. Increasing flow velocity decreases the boundary layer resistance in the liquid phase, and consequently decreases the term $1/k_m a_v$, and increases the overall rate constant k^*. The effect of the liquid flow velocity in the range 2.31–6.94 cm min^{-1} on the overall removal efficiency and rate constant is shown in Figure 6b. As stated earlier the effective length of the column where light transmission was occurring from the coated fiber in a channel was only 5 cm although the total fiber length was 30 cm. Thus the mass transfer coefficients are based on the 5 cm effective length. Both PHE and DCB showed similar trends. The conversion decreased as flow velocity increased (Figure 6a). This is because increasing flow velocity decreases the residence time for a given reactor length and hence the overall conversion of PHE and DCB decrease. However, as

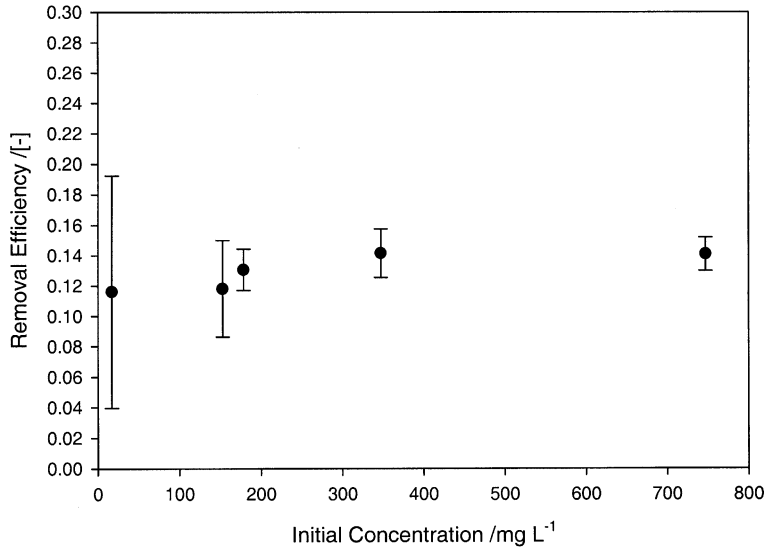

Fig. 5. The effect of initial feed PHE concentration on the removal efficiency. The flow velocity was 2.87 cm min^{-1}; the fibers were coated with 0.25 wt. % TiO_2 slurry solution.

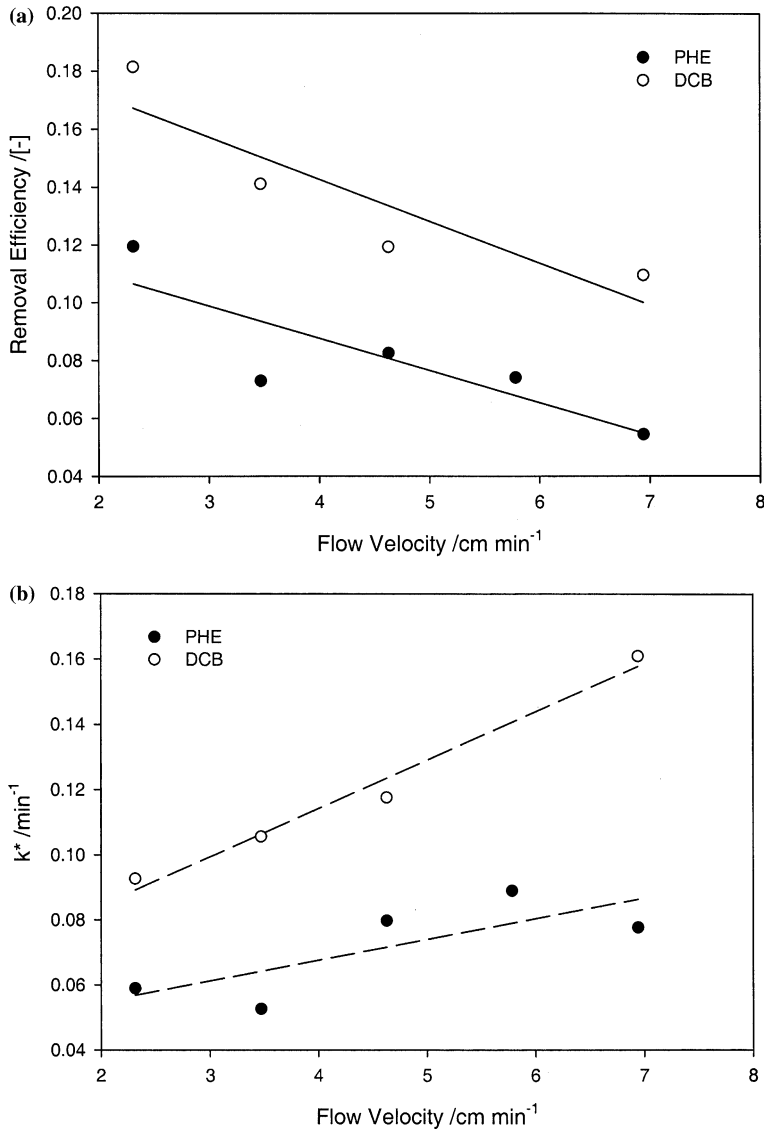

Fig. 6. The effect of the liquid flow velocity on (a) the overall removal efficiency and (b) rate constant for DCB and PHE in the monolith reactor. The optical fibers were coated with 0.25 wt. % TiO_2 slurry solution.

shown in Figure 6b, the overall rate constant, k^*, increased linearly with increasing flow velocity. This means the monolithic reactor was operated in the mass transfer control regime, which lowered the overall degradation efficiency.

3.5. *Effects of coating thickness on optical fiber*

In each channel of the monolith photocatalytic reactor, the catalyst can be immobilized either on the outer surface of the optical fiber or on the inner surface of the monolith channel. In the former case, the catalyst is illuminated by an immersion-type light source, which is the fiber quartz core. In the latter case, the fiber can be treated as an external-type light source, i.e., light has to travel through the absorbing liquid medium and then falls on the catalyst surface. Chen et al. [33] depicted these two circumstances as substrate–catalyst (SC) and liquid–catalyst (LC) illumination, depending on whether the catalyst is activated from the substrate side or from the liquid side.

In the monolithic reactor, the surface area of the TiO_2 layer on the channel wall is much larger than that of the TiO_2 layer on the fiber (7.5 times larger considering the diameter of the fiber is 0.4 mm and that of the channel is 3 mm), thus ensuring that a strong enough UV light reaching the TiO_2 layer on the channel wall is the likely key to increase illuminated active catalyst surface area in a given reactor volume for the monolith reactor design. The direction of incident light and the diffusion of reactants onto the TiO_2 layer on the fiber are opposite whereas the directions are the same onto the TiO_2 layer on the wall of the channel. Based on Beer's law, the refracted light intensity is exponentially extinguished when penetrating the TiO_2 layer. The penetration depth was estimated to be 1.7–3.3 μm [22] or up to 5 μm [33], which depends on the characteristic of the catalyst and the porosity of the film. For LC illumination, incident

light always penetrates from the outer layer of the TiO_2 film and the active catalysts are always close to the liquid–catalyst interface. Therefore internal mass transfer is not a problem in this case. However, SC illumination is much different. When the direction of the light penetration and the reactant diffusion are opposite, light cannot penetrate through the thick TiO_2 layer and thus the active catalyst is far from the liquid-catalyst interface. Consequently, the reactants have to diffuse into the pores of the TiO_2 layer and then have a chance to contact the active catalyst. Thus internal mass transfer can be rate controlling, since the pores of the TiO_2 layer are very small. A thickness the same as the penetration depth was claimed to be optimum for the OFR reactor [21]. However, in our reactor design, a thick TiO_2 layer on the optical fiber should be avoided in order to illuminate the catalyst surface on the channel wall. The desired thickness of the TiO_2 layer on an optical fiber should be less than the penetration depth.

As shown in Figure 7, the thickness of the TiO_2 film coated on the optical fiber affects the overall PHE and DCB rate constant. Both the PHE and DCB overall rate constant reach the highest value when the thickness of the optical fiber is around 0.4 μm, which is comparable to the wavelength of the UV-A light. The overall rate constants decreased dramatically for coating layers greater than 0.4 μm. If the thickness of a TiO_2 film is smaller than the wavelength, the film can barely absorb the light. When the thickness was equal to the UV-A wavelength, the TiO_2 film absorbed 10% of the incident light on the optical fiber; the remaining 90% of the light penetrated the bulk solution and was absorbed by the TiO_2 coating on the monolith channel wall. Since the available catalyst surface on the channel wall is 7.5 times larger than that on the optical fiber, decreasing the light intensity on the catalyst layer on the channel wall could decrease the overall reaction rate substantially.

We observed from Figure 7 that even though the optical fibers were not coated with TiO_2 layer, some extent of photocatalytic degradation still existed, which contradicts the assumption of the total reflection of UV light inside the bare quartz fiber core without TiO_2 film immersed in the aqueous solution. This is because the surface of the bare optical fiber core was roughened by sandpaper treatment. The roughness of the interface between quartz and water can either increase or decrease the incidental angle. Thus the light rays whose incidental angles were larger than the critical angle leaked out of the fiber. The leaking light then penetrated the aqueous solution and illuminated the surface of the TiO_2 film on the monolith channel. These illuminated active catalyst sites contributed to the photodegradation of the organic compounds.

3.6. *Comparison of different reactor designs*

Quantum efficiency (Φ), which is used to evaluate the efficiency of the photocatalytic reactor, is defined as the number of molecules N_{mol} undergoing an event (conversion of reactants or formation of products) relative to the number of quanta N_{photon} absorbed by the reactants or by the photocatalyst:

$$\Phi \equiv \frac{N_{mol}(\text{mol/s})}{N_{photon}(\text{einstein/s})} = \frac{\text{rate of reaction}}{\text{rate of photon absorption}} \tag{10}$$

However, the number of absorbed photons is hard to assess owing to the optical effects, such as reflection, scattering and transmission on the photocatalyst and support. Moreover, it is the total energy consumption, not just the absorbed optical energy, which would be an indicator of the operation cost to evaluate the economic efficiency of a photocatalytic reactor. Therefore, the usage of the term apparent quantum efficiency

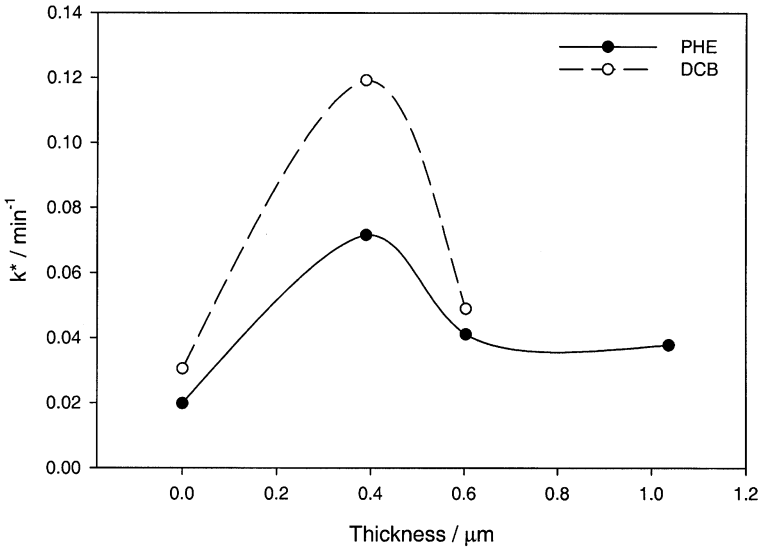

Fig. 7. The effect of thickness of the TiO_2 film coated on the optical fiber on the overall rate constant.

Table 1. Comparison of photocatalytic reactors

	Slurry reactor	Continuous annular reactor	Optical fiber monolith reactor
Reactor volume (ml)	5	8.1	21.3[a]
Mode of reactor operation	Batch	Continuous	Continuous
Illuminated catalyst surface area per unit volume of liquid treated inside the reactor ($m^2\ m^{-3}$)	39,473[b]	141	1538
Apparent rate constant, k^* (min^{-1})	–	DCB: 0.015–0.035 PHE: 0.10–0.17	DCB: $4.0 \sim 4.5 \times 10^{-2}$ PHE: $5.3 \sim 8.9 \times 10^{-2}$
Apparent quantum efficiency	DCB: $7.2 \sim 52 \times 10^{-5}$	DCB: $2.8 \sim 4.7 \times 10^{-4}$ PHE: $3.7 \sim 27 \times 10^{-5}$	DCB: 0.045 PHE: $2.2 \sim 3.3 \times 10^{-3}$
Scale-up possibility	No	No	Yes

[a]Based on an effective reactor length, which is 5 cm.
[b]The value will be much lower than 39,473 $m^2\ m^{-3}$ as most of the suspended catalyst particles are not effectively illuminated.

referenced to incident photons in heterogeneous photocatalysis was proposed at 365 nm.

$$\Phi_a = \frac{\text{rate of reaction}}{\text{flux of incident photons}} \cong \frac{k^* C_0 V}{I_i A / U_{\lambda=365\,\text{nm}}} \tag{11}$$

where V is the volume of treated water solution in the monolith reactor; A is the illuminated area of the fiber tips; $U_{\lambda=365} = 3.28 \times 10^5$ J Einstein^{-1} is the energy of 1 molar photons at wavelength $\lambda = 365$ nm. All of the incident photons entering the upper fiber tips were treated as absorbed photons on TiO_2 layers without attenuation. Obviously, the apparent quantum efficiency should be lower than the actual quantum efficiency.

Table 1 compares the optical fiber monolith reactor (OFMR) with the batch slurry reactor and the continuous annular reactor (CAR) in our previous study. Based on our calculation, we observed an increase of about an order of magnitude for the illuminated catalyst surface area per unit volume of liquid treated inside the OFMR when compared with the CAR or the OFR reactor. At the flow velocity range of 2–8 cm min^{-1} and an initial concentration of 500μg l^{-1} for PHE, the apparent quantum efficiency of the optical fiber monolithic reactor is much greater than that of the continuous annular reactor. For DCB at an initial concentration of 17 mg l^{-1} and at similar flow conditions, the apparent quantum efficiency is about 2 orders of magnitude greater compared with the annular reactor. All of these observations suggest the highly promising nature of the optical fiber monolith reactor in photocatalysis.

4. Conclusions

A laboratory-scale optical fiber monolithic reactor was designed, constructed and tested with two model compounds (DCB and PHE) for overall performance evaluation. Experimental results showed two orders of magnitude higher apparent quantum efficiency compared with the continuous annular reactor, which suggested an appropriately designed optical fiber monolithic reactor could have potential in photocatalytic water treatment. The effects of initial feed concentration, flow velocity (mass transfer), and the thickness of the TiO_2 layer on the optical fiber were investigated. The results showed the operation fell in the mass transfer regime due to the narrow flow passage in each cell of the monolith. Further research should improve the mass transfer limitations either by increasing the flow velocity or changing the reactor column operation mode from the present fix-bed type to a trickle-bed type. Thin TiO_2 film on the optical fiber is required in this configuration to prevent the light from total reflection inside the fiber core and facilitating light penetration through the TiO_2 layer. The optimum thickness of the TiO_2 film on the optical fiber was about 0.4 μm in this study. Thick TiO_2 film was formed on the monolith channel wall to fully absorb the incident UV light. In the present study, the short light propagating length (5–6 cm in this study), which significantly limits the efficient use of optical fibers, should be overcome. Subsequent research work will extend the light propagating length either by increasing the diameter of optic fibers or depositing non-homogenous TiO_2 coating on the optical fibers.

Acknowledgment

This work was supported by a grant from the U.S. EPA through the Gulf Coast Hazardous Substance Research Center, Lamar University, TX.

References

1. A. Mills, R.H. Davies and D. Worley, *Chem. Soc. Rev.* **22** (1993) 417.
2. O. Legrini, E. Oliveros and A.M. Braun, *Chem. Rev.* **93** (1993) 671.
3. M.R. Hoffmann, S.T. Martin, W.Y. Choi and D.W. Bahnemann, *Chem. Rev.* **95** (1995) 69.
4. A Mills and S.J. LeHunte, *J. Photochem. Photobiol. A* **108** (1997) 1.
5. J.M. Herrmann, *Catal. Today* **53** (1999) 115.
6. O.M. Alfano, D. Bahnemann, A.E. Cassano, R. Dillert and R. Goslich, *Catal. Today* **53** (2000) 199.

7. A.K. Ray, *Chem. Eng. Sci.* **54** (1999) 3113.
8. H. Al-Eekabi, M.A. Anderson, H. Kikkawa, M. Edwards and C.G. Hill, *J. Catal.* **127** (1991) 167.
9. S. Naskar, S.A. Pillay and M. Chanda, *J. Photochem. Photobiol. A.* **113** (1998) 257.
10. A.K. Ray and A.A.C.M. Beenackers, *AIChE J.* **44**(2) (1998) 477.
11. M. Bideau, B. Claudel, C. Dubien, L. Faure and H. Kazousan, *J. Photochem. Photobiol. A* **91** (1995) 137.
12. Y. Zhang, J.C. Crittenden, D.W. Hand and D.L. Perram, *Environ. Sci. Technol.* **28** (1994) 435.
13. G. Chester, M. Anderson and H. Read, *J. Photochem. Photobiol. A.* **71** (1993) 291.
14. H. Al-Ekabi, A. Safazadey-Amiri, W. Sifton and J. Story, *Int. J. Environ. Pollut.* **1** (1991) 125.
15. R.E. Marinangeli and D.F. Ollis, *AIChE J.* **23** (1977) 415.
16. R.E. Marinangeli and D.F. Ollis, *AIChE J.* **26** (1980) 1000.
17. R.E. Marinangeli and D.F. Ollis, *AIChE J.* **28** (1982) 945.
18. K. Hofstadler, R. Bauer, S. Novalic and G. Heisler, *Environ. Sci. Technol.* **28** (1994) 670.
19. N.J. Peill and M.R. Hoffmann, *Environ. Sci. Technol.* **29** (1995) 2974.
20. N.J. Peill and M.R. Hoffmann, *Environ. Sci. Technol.* **30** (1996) 2806.
21. N.J. Peill and M.R. Hoffmann, *Environ. Sci. Technol.* **32** (1998) 398.
22. W. Choi, J.Y. Ko, H. Park and J.S. Chung, *Appl. Catal. B* **31** (2001) 209.
23. W. Wang and Y. Ku, *J. Photochem. Photobiol. A* **159** (2003) 47.
24. W.R. Moore, R.P. Richmond, G.L. Vaneman and D. Dou, *Evaluation of High Cell Density Substrates for Advanced Catalytic Converter Emissions Control* (SAE International, Warrendale, PA, 1999)1999-01-3630.
25. M.L. Sauer and D.F. Ollis, *J. Catal.* **149** (1994) 81.
26. M.M. Hossain and G.B. Raupp, *AIChE J.* **45** (1999) 1309.
27. G.B. Raupp, A. Alexiadis, M.M. Hossain and R. Changrani, *Catal. Today* **69** (2001) 41.
28. G.S. Son, S.W. Yun, S.H. Ko, J.W. Song and K.Y. Lee, *J. Adv. Oxid. Technol.* **6** (2003) 80.
29. H.F. Lin and K.T. Valsaraj, *Sep. Purif. Technol.* **28** (2002) 87.
30. H.F. Lin and K.T. Valsaraj, *J. Hazard. Mater. B* **99** (2003) 203.
31. V. Balakotiah, N. Gupta and D.H. West, *Chem. Eng. Sci.* **55** (2000) 5367.
32. C.F. Turchi and D.F. Ollis, *J. Phys. Chem.* **92** (1988) 6852.
33. D. Chen, F. Li and A.K. Ray, *AIChE J.* **46** (2000) 1034.